A Beamformer to Play with Wall Reflections: The Icosahedral Loudspeaker

Franz Zotter,* Markus Zaunschirm,* Matthias Frank,* and Matthias Kronlachner†

*Institute of Electronic Music and Acoustics
University of Music and Performing Arts
Inffeldgasse 10/3
8010 Graz, Austria
{zotter, zaunschirm, frank}@iem.at
†Automotive Systems GmbH
Harman Becker
Schlesische Str. 135
94315 Straubing, Germany
matthias.kronlachner@harman.com

Abstract: The quote from Pierre Boulez, given as an epigraph to this article, inspired French researchers to start developing technology for spherical loudspeaker arrays in the 1990s. The hope was to retain the naturalness of sound sources. Now, a few decades later, one might be able to show that even more can be done: In electroacoustic music, using the icosahedral loudspeaker array called IKO seems to enable spatial gestures that enrich alien sounds with a tangible acoustic naturalness.

After a brief discussion of directivity-based composition in computer music, the first part of the article describes the technical background of the IKO, its usage in a digital audio workstation, and psychoacoustic evidence regarding the auditory objects the IKO produces. The second part deals with acoustic equations of spherical beamforming, how the IKO's loudspeakers are controlled correspondingly, how we deal with excursion limits, and the resulting beam patterns generated by the IKO.

> The loudspeaker "anonymizes" the actual source. . . . There will be more resemblance, in a certain way, between amplified piano and amplified harp, than between amplified and unamplified piano. One could say that the instruments have gone through a "rolling mill" of amplification and have lost some of their individuality. . . . The composer is left to play with this phenomenon and to make use of it in an informed manner.
>
> —Boulez 1983

Composing Directivity for Electroacoustic Music

In electroacoustic music, we find the application of directionality in Marco Stroppa's music that used vertically stacked loudspeakers, each of which was aimed at a different angle. These were called *totem acoustiques*, and were used in his compositions *. . . of Silence* (2007), *Hist Whist* (2009), and most prominently in the opera *Re Orso* (2011) with an eight-loudspeaker column hanging in the middle of the stage.

A starting point to composing with directivity is "La Timée," a cube housing six loudspeakers utilized by the researchers at IRCAM in order to give more naturalness to loudspeaker-based diffusion of sounds (Caussé, Bresciani, and Warusfel 1992; Warusfel, Derogis, and Caussé 1997; Misdariis et al. 2001).

The playback system discussed here, called IKO, is a 20-sided, 20-channel loudspeaker system in the form of the convex regular icosahedron (see Figure 1). As a compact spherical loudspeaker array, the IKO provides the technical means to project a focused sound beam in a freely adjustable direction. Inside a room, this kind of beam direction can be set to predominantly excite selected wall reflections, or combinations of reflections, causing interesting effects in perceived localization.

Although the beamforming of the IKO is capable of uniform adjustment to all directions, contiguous directions are not mapped to contiguous perceived directions, as reflection paths of a room are discrete. Still, the IKO's sculptural auditory objects

Computer Music Journal, 41:3, pp. 50–68, Fall 2017
doi:10.1162/COMJ_a_00429

Figure 1. The IKO is a 20-sided, 20-channel loudspeaker array in the form of an icosahedron. Its diameter is about 60 cm.

(cf. Sharma 2016) offer an exciting spatialization technology to composers of electroacoustic music, in the broadest sense of the term. The IKO's presence on stage offers a scene that is unexpectedly pronounced and natural, like that of a human performer.

We promote the use of variable directivity of compact spherical loudspeaker arrays in computer music to create new auditory objects. The first half of this article is dedicated to the existing software solutions to working with the IKO, the IKO's hardware, its staging, and what is known about the perception of its sound beams in a room. The second half provides a deeper understanding of the acoustic principles behind the IKO's spherical beamforming, an approach to stay within excursion limits of the transducers, and details on how the spherical beamforming and velocity control of the IKO are achieved and verified, on the basis of measurements and a multiple-input, multiple-output (MIMO) system design.

Part I: Beamforming and the IKO in Practice

The first half of this article deals with a literature review on beamforming, beamforming applications, and compact spherical loudspeaker arrays, and information about the IKO that is relevant for its practical application—how it is controlled with plug-ins for a digital audio workstation (DAW), how it is virtualized for different rooms using binaural synthesis, what it is built of, how it can be presented and staged, and which auditory objects can be expected from the existing perceptual studies.

Technical Background and Literature

Classical beamforming technology aims at focused emission and reception of waves by arrays of transducers driven and superimposed with different weights, delays, or filters. If beamforming only uses delays or weights, we speak of *delay-and-sum* or *weight-and-sum* beamforming, respectively, whereas the most general approach using filters is called *filter-and-sum* beamforming (Schelkunoff 1943; Brandstein and Ward 2001). When allowing filters with gains exceeding the maximum of the directivity pattern, strong focusing is possible even with small apertures. This is called *superdirective* or *supergain* beamforming (Bloch, Medhurst, and Pool 1953; Elko 2000).

Based on the idea of exploiting beamforming to selectively excite wall reflections as a type of surround-sound technology, a planar loudspeaker array at the typical center loudspeaker position is commercialized in Yamaha's Sound Bar for home-cinema applications (Takumai 2006). In this application, surround and side loudspeakers are substituted by beams emphasizing suitable wall reflections.

As an alternative method of creating strongly focused sound beams, parametric arrays utilize the nonlinearity of air (Bennett and Blackstock 1975; Croft and Norris 2003). A powerful group of ultrasound transducers plays an amplitude-modulated carrier frequency above 35 kHz at a sound pressure level higher than 120 dB. Its envelope is demodulated along the propagation path. The interpretation as a nonlinear source phenomenon is called a *parametric array*. Sugibayashi et al. (2012) built and evaluated the use of directionally adjustable ultrasound transducer arrays mounted on each of the 20 surfaces of an icosahedron to establish a mixed-reality sound-field synthesis. This intriguing system had to be supplemented, however, by common electrodynamic transducers to support frequencies below 1 kHz.

The technology utilized for compact spherical loudspeaker arrays such as the IKO is linear and superdirective, and is called *spherical harmonic beamforming* (cf. Butler and Ehrlich 1977 for underwater sound and Warusfel, Derogis, and Caussé 1997 for music). The targeted directional resolution is uniform and independent of the beam direction, and the technique is based on filtering to equalize different attenuations for spherical harmonics of different orders, when radiated to the near or far field (Zotter and Noisternig 2007).

The reasoning behind a variable-directivity playback device for music (as presented by Caussé, Bresciani, and Warusfel 1992; Warusfel, Derogis, and Caussé 1997; Misdariis et al. 2001) has motivated other research groups to pursue technical efforts of establishing and controlling compact spherical loudspeaker arrays. At Princeton University, arrays like these have been built for electroacoustic performances with, for instance, the Princeton laptop orchestra (Cook et al. 1998; Trueman et al. 2006). At the University of California, Berkeley, researchers investigated magnitude-based beam-pattern control and accuracy limits (Kassakian and Wessel 2003, 2004; Kassakian 2005, 2006; Avizienis et al. 2006). Further notable efforts to build, control, and use arrays such as these have been undertaken in Austria (Zotter and Höldrich 2007; Zotter and Noisternig 2007; Pomberger 2008; Zotter, Pomberger, and Schmeder 2008; Zotter 2009; Kerscher 2010; Zotter and Bank 2012), Germany (Pollow and Behler 2009; Pollow 2014), Brazil and France (Pasqual 2010; Pasqual, Herzog, and Arruda 2010; Pasqual, Arruda, and Herzog 2010), Israel (Rafaely and Kaykin 2011; Morgenstern, Zotter, and Rafaely 2012; Morgenstern, Rafaely, and Zotter 2015), Australia (Miranda, Cabrera, and Stewart 2013), and New Zealand (Poletti, Betlehem, and Abhayapala 2015).

Other work has been pursued recently in our present research project Orchestrating Space by Icosahedral Loudspeaker (OSIL), for which the goal is to artistically find and define sound sculptures by composing music with the IKO (Sharma 2016) and to scientifically investigate these sculptures (Sharma, Zotter, and Frank 2014; Frank, Sharma, and Zotter 2015; Wendt et al. 2016, 2017; Zaunschirm, Frank, and Zotter 2016).

Controlling the IKO with DAW Plug-ins

Real-time performances and composition for the IKO can be controlled from a standard consumer personal computer, or even a laptop. The 20 driving signals for the IKO's loudspeakers are generated using a combination of the ambiX and mcfx VST plug-ins (Kronlachner 2014), see Figure 2. The ambiX software allows one to create, modify, and decode higher-order Ambisonics on a DAW. Although Ambisonics is usually associated with loudspeakers surrounding the audience, the same representation is deployed to control directional beams radiated outwards from compact spherical arrays such as the IKO.

Care has been taken to make the required matrix convolution efficient, as the IKO's control system (see Figure 3) consists of 320 FIR filters (20 channels, each requiring 16 filters) whose coefficients are stored as WAV files. The mcfx_convolver software carries out convolutions as nonuniform, partitioned fast convolutions for low latency and low CPU load. The filters used by mcfx_convolver to connect each of its inputs to each of its output is specified in a configuration file. Selecting from different configuration files allows performance with different setups—for instance, on a different array or with a different filter set. To host the ambiX and mcfx VST plug-ins, DAWs and other music software environments, such as Max, AudioMulch, Bidule, Ardour, and Reaper, must be capable of dealing with at least 20 channels. For the IKO, we mainly use Reaper because of its support for up to 64 channels per track or bus. Furthermore, it supports live performance and improvisation by remote control using Open Sound Control (OSC). Other convenient features include the ability to record and program automations, as well as faster-than-real-time rendering of finished projects to 20-channel audio files. Reaper and the plug-ins are available under Windows, Mac OS, and Wine (Linux).

The signal routing and processing schema is shown in Figure 3. A playback signal $s_c(t)$ and

Figure 2. Screenshots of VST plug-ins controlling the IKO. The plug-in ambix_encoder_o3 (a) controls the beam direction of the IKO for one input signal by encoding it to 16 third-order Ambisonic signals. The plug-in mcfx_convolver24 (b) generates 20 loudspeaker signals from the 16 third-order Ambisonic signals using real-time convolution.

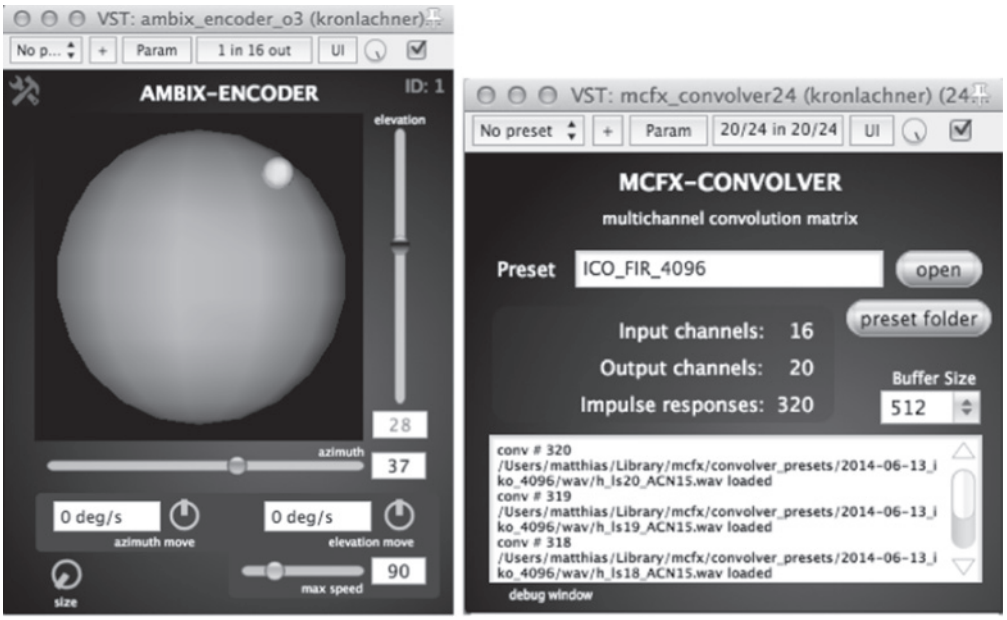

(a) (b)

Figure 2

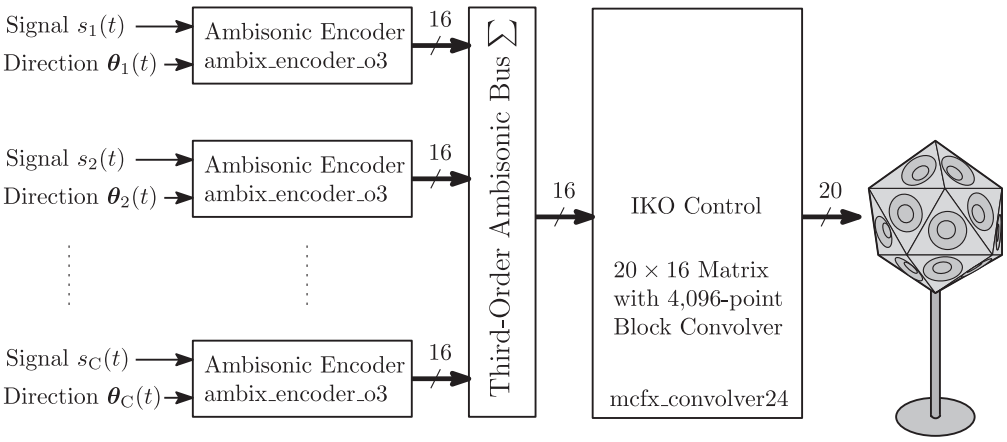

Figure 3

its beam direction $\boldsymbol{\theta}_c(t)$ are fed into a third-order Ambisonics encoder as an insert effect (ambix_encoder_o3). The resulting 16 channels are sent to a master mix. The 20-channel master mix uses a 20×16 fast convolution matrix as an insert effect (mcfx_convolver24), with 4,096 coefficients at a sample rate of 44.1 kHz. The resulting 20 signals feed the amplifiers for the 20 loudspeakers of the IKO. In the real-time operation of the IKO, CPU load amounts to 65 percent for ten sources and a 512-sample buffer, using a MacBook Pro 2.53 GHz Intel Core 2 Duo.

Figure 4. Processing schema of the virtual IKO using measured room impulse responses from the IKO to the Eigenmike EM32 and measured HRIRs.

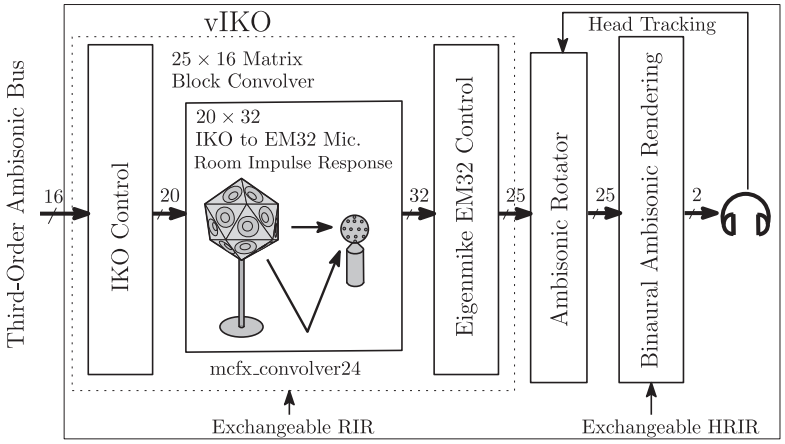

The Virtual IKO for Headphones

The virtual IKO (vIKO) by Zaunschirm, Frank, and Zotter (2016) provides a DAW-based real-time simulation of the IKO by binaural synthesis to headphones, optionally head-tracked (see Figure 4). It provides a Reaper session with suitable routing and delivers a collection of presets for the aforementioned plug-in suites. The presets provided are based on measurements taken in different rooms using the IKO as a source and using the Eigenmike EM32 to capture impulse responses at different listening positions. The vIKO comes with two exemplary room responses and, currently, two sets of head-related impulse responses (HRIRs) measured by the Acoustics Research Institute in Vienna. Each of these sets can be chosen for matrix convolution in the mcfx_convolver plug-in and for binaural rendering in the ambix_binaural plug-in, respectively. Based on vIKO, the OSIL Web site (http://iem.at/osil) offers binaural renderings of basic time-variant beam constructions (called IKO moves) and of musical pieces.

IKO Hardware

The IKO turned out to perform well in electroacoustic concerts thanks to its large and powerful transducers. By contrast, the transducers described in the initial technical report by Zotter and Sontacchi (2007), or smaller arrays such as the prototype by Kerscher (2010), were not powerful enough for concert performances. The IKO is constructed of 20 equilateral triangular faces with 34.7-cm-long outer edges, made from medium density fiberboard, and cut with a bevel of 20.9°. Ten of these faces are glued together in the shape of two pentagonal pyramids of five triangular faces each. The apexes of the two pyramids form the upper and lower apex of the IKO. They are twisted 36° with respect to each other, and they are glued to a horizontal belt of ten faces pointing upward and downward in alternation (cf. Figure 5a). The interior of the IKO is a

Figure 5. Measurement setups for loudspeaker cone velocity and sound pressure: laser vibrometer measurement of voltage-to-loudspeaker cone-velocity transfer functions (a) and sound pressure measurement with semicircular microphone array (r = 75 cm) at IEM CUBE, with a turntable so that directivity is measured at 18 × 36 = 648 directions (b).

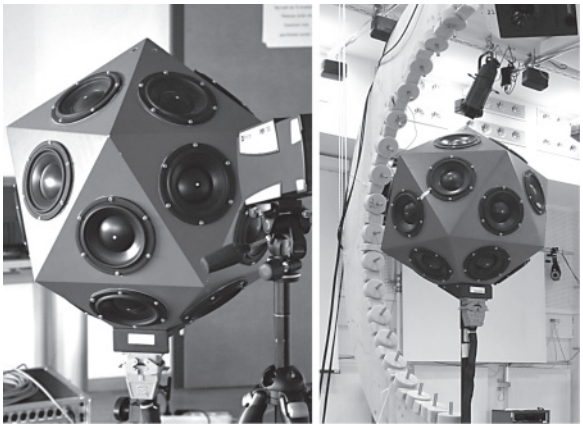

(a) (b)

Figure 5

Table 1. Azimuth and Zenith Angles for IKO Loudspeakers

Loudspeaker	*Azimuth*	*Zenith*	*Loudspeaker*	*Azimuth*	*Zenith*
1	0°	142.62°	11	36°	79.19°
2	72°	142.62°	12	108°	79.19°
3	144°	142.62°	13	180°	79.19°
4	−144°	142.62°	14	−108°	79.19°
5	−72°	142.62°	15	−36°	79.19°
6	0°	100.81°	16	36°	37.38°
7	72°	100.81°	17	108°	37.38°
8	144°	100.81°	18	180°	37.38°
9	−144°	100.81°	19	−108°	37.38°
10	−72°	100.81°	20	−36°	37.38°

Loudspeaker 1 is next to the cable socket, the sequence runs counterclockwise from bottom to top.

single unpartitioned volume filled with wool, and it contains the cabling of the transducers, which is attached to the back of a 42-pin Harting Han DD industrial socket. In the center of each of the 20 faces, a 6.3-in. Morel CAW-638 transducer is mounted and can produce an excursion of up to $x_{max} = \pm 4.25$ mm. The channel indices and angular coordinates of the loudspeakers are given in Table 1. The Harting socket on the outside allows one to attach a cable hanging downwards, which is a 15-m-long bundle of 20×1.5-mm^2 loudspeaker wire pairs gathered in a braided sleeving. At the other end, the cables are attached to a socket connected to the 40 banana-jack sockets of a customized sonible d:24. This is a compact 24-channel amplifier consisting of three rack units with 250 W per channel.

The prototype of the IKO, developed at the Institute of Electronic Music and Acoustics (IEM) and described in this article, was used for measurements, experiments, performances, etc., leading to a cooperation with the company sonible to manufacture the IKO and market it commercially (cf. http://iko.sonible.com). This new IKO by IEM and sonible is redesigned for easier transport and for easy integration with the MADI/Dante-capable sonible d:24 multichannel amplifier. It uses a newer Morel transducer series ensuring high performance.

Staging the IKO

The IKO can create auditory objects of high spatial definition when utilizing first-order reflections of the walls in the performance space. In current performance practice, two basic staging constellations are used: one for typical rectangular rooms, and another that uses a concave setup of reflectors behind the IKO (Sharma 2016; see also Figure 6).

Rectangular rooms are the simplest constellation in which the IKO is played, preferably between a corner of the room and the audience. This was the constellation used, for instance, in concerts showcasing IKO held at the International Conference on Digital Audio Effects (DAFx) in 2010, at the Darmstadt International Summer Courses for New Music in 2014, and in the Media Art Gallery at the Zagreb Showroom of Contemporary Sound (Izlog Suvremenog Zvuka) festival in 2015. This arrangement makes it possible to exploit balances between at least two pronounced reflections from the walls and the direct sound. The IKO's distance to the audience should be at least as far as the distance to both walls. Rectangular rooms often offer more effects, such as usable reflections, for example, at the ceiling, at the floor, or from a more distant side wall, as well as spatial reverberation effects. There is, however, some risk depending on the geometry, wall material, sound material, etc. It is therefore

(a) (b)

Figure 6. IKO in the performance setup in MUMUTH, Graz, at the 2010 International Conference on Digital Audio Effects (a), and in the ZKM Kubus, Karlsruhe, at the 2015 InSonic festival (b).

wise to compose pieces that can be adjusted to the given environment.

Alternatively, concave arrangements of reflectors behind the IKO were used at a concert in the Signale Graz festival in 2014 and at the InSonic conference held at ZKM in 2015 (see Figure 6), offering a large set of useful, distinct reflections. We had a similar performance situation in the French Pavilion at the Showroom of Contemporary Sound festival in 2015, where the cylindrical wall of the performance space could be used without modification. The concave reflector arrangement behind the IKO should preferably exhibit a radius of about 5 m to 7 m, and the loudspeaker should be placed in the symmetry axis of the arrangement at a distance of about 1.5 m to 3 m. The concave setup increases the number of reflections (stage wall, side walls), which are otherwise limited, to a plethora of distinct reflections, available everywhere between the stage and the side walls. The audience should preferably be at least about 5 m away from the IKO to allow a balanced perspective on auditory objects that can be shaped by the reflections.

At the low-frequency end (less than 100 Hz), the IKO is omnidirectional and acts as a powerful subwoofer that is well able to excite large spaces. In the octave above 100 Hz, beams radiated by the IKO become directional, so that bass in the octave above 100 Hz can be moved around in the room. Such sounds are often localized as rotary spacious zones that are not colocated with the IKO.

Perception of Sound Beams in Rooms

Although it might seem logical that the sound propagation path emphasized the most would appear as a localized direction in our perception, the precedence effect counteracts this intuition. To study the perceived localization of directional sources with variable orientation, our initial studies (Zotter et al. 2014; Zotter and Frank 2015) considered a simulated source with a third-order beam pattern in a rectangular room. Third-order beam patterns are composed of all spherical harmonics of the orders $n = 0 \ldots 3$. Direct and reflected sound were simulated using the image-source method up to first and second order, which were auralized on 24 Genelec 8020 loudspeakers arranged on a horizontal ring in an anechoic environment.

The first of these two studies showed that the orientation of directional sound sources can be perceived, with a localization that can substantially deviate from the direct path. It used nine volunteer listeners who undertook the task of localizing test signals consisting of bursts of pink noise. The localized direction could be modeled (1) by an extended energy-vector model considering a rough echo threshold of −0.25 dB/ms (Rakerd, Hartmann, and Hsu 2000) and (2) by a binaural predictor based on a model proposed by Werner Lindemann (1986).

The second study, with eleven experienced volunteer listeners with normal hearing, was also based on an auralized source with third-order beam patterns

and tested the perceived direction localization for 36 source orientations in 10° steps. Each listener was presented with conditions in individual random sequence and could respond not only by a single, primary localization direction, but also by a possible secondary one. Listeners were asked to respond by naming integers, based on the even-numbered ticks visibly attached to the loudspeakers. The primary direction could be modeled by the aforementioned extended energy-vector. Secondary directions appeared to be difficult to model and were perceived in only 24 percent of the 36 source orientations using auralization with direct sound and first-order image-sources, but in 42 percent with second-order image sources added, indicating a dependency on later reflections. By contrast, primary localization directions were not changed much by second-order image sources.

Apart from perceived direction, the perceived distance when using a source with controlled directivity has also been investigated (Laitinen et al. 2015; Wendt et al. 2016). Wendt and colleagues described the relation between perceived distance and beam-pattern control such as beam width (i.e., order) or the angle between a pair of symmetric third-order beams.

Wendt and coworkers (2017) provided a collection of formal listening experiments with the physical IKO's spherical harmonic beamforming in a real room. These experiments test (1) the localization of static beam directions, (2) the localization of time-variant beam steering using different sounds, and (3) whether "sculptural" compositional categories can be distinguished based on spatial impressions, as opposed to impressions based on monophonic playback.

From Wendt et al.'s second experiment, we can present further results demonstrating that beamforming from the physical IKO in a physical room (which is not ideal) is able to influence the impression of distance in the case of time-varying beam-pattern control (for details of the acoustical properties and the exact setup positions of the experiment, cf. Wendt et al. 2017). Fifteen listeners with experience in auditing spatial audio, drawn from IEM's expert listening panel, took part in the experiment, in which each listener gave responses for two listening positions.

The conditions consisted of 5 sec of pink-noise bursts and a 5-sec, time-varying beam-pattern control. Subjects were asked to mark the position of the evoked auditory object in time steps of 0.5 sec, using ten controllable dots on a graphical interface showing the layout of both the room and IKO (cf. Figure 7). Each of the dots could be moved by mouse and flashed at the corresponding moment of playback. Listeners could repeat the playback until they were satisfied with the match of their response and what they perceived.

Binaural renderings using vIKO (Zaunschirm, Frank, and Zotter 2016) are available online: http://phaidra.kug.ac.at/o:37710, http://phaidra.kug.ac.at/o:37712 for the two beam-pattern-control conditions at position 1, and http://phaidra.kug.ac.at/o:37711, http://phaidra.kug.ac.at/o:37711 for position 2.

Figure 7 shows the mean results for each time step for two beam-pattern control conditions: (1) left–right amplitude panning from a beam aiming toward the left to a beam aiming toward the right, (2) distance panning for beam steering to the back wall (i.e., direct sound at listening position 1). The distance panning gradually changes the order of the beam pattern from third order to zeroth order and back again to third order. Distance panning works more clearly at position 1, but also affects the perceived location at position 2. The result for left–right amplitude-panned beam pairs is perceivable from both listening positions and indicates the feasibility of lateral distance control for auditory events created by the IKO.

Part II: Beamformer Theory and Control of the IKO

Based on the technical background provided in Part I, we now look to a deeper understanding of the working principles behind beams formed with compact spherical loudspeaker arrays such as the IKO. It explains the governing acoustic equations in general, and for the IKO as a particular case. A comprehensive approach is outlined for the design

Figure 7. Geometry of the experiment, showing the listening and IKO positions in our lecture room for listening positions 1 (a) and 2 (b). Dark gray circles indicate mean localized positions for distance panning, and light gray squares the positions for left-right panning. Marker size increases with time.

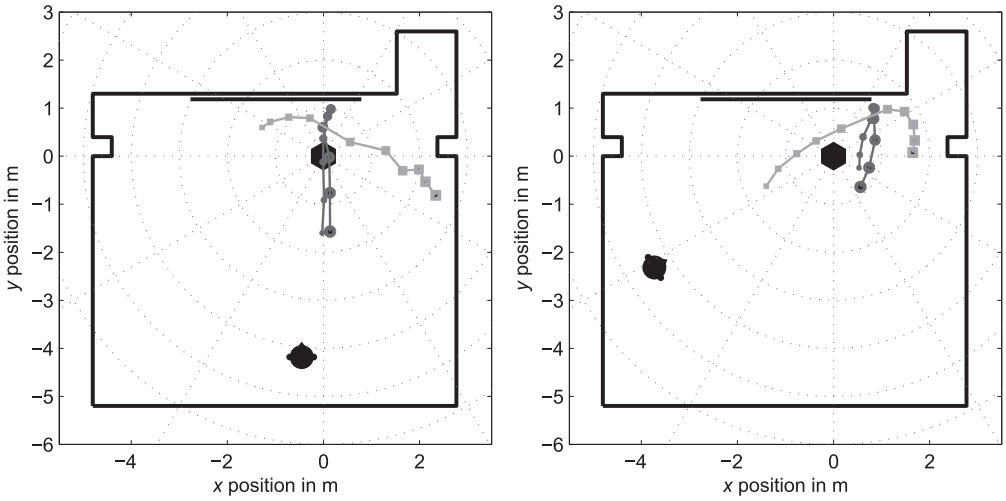

Figure 7

Figure 8. Spherical harmonic patterns up to third order (a). Specific surface vibration patterns (b) can synthesize spherical harmonic beam patterns in the far field (cap model).

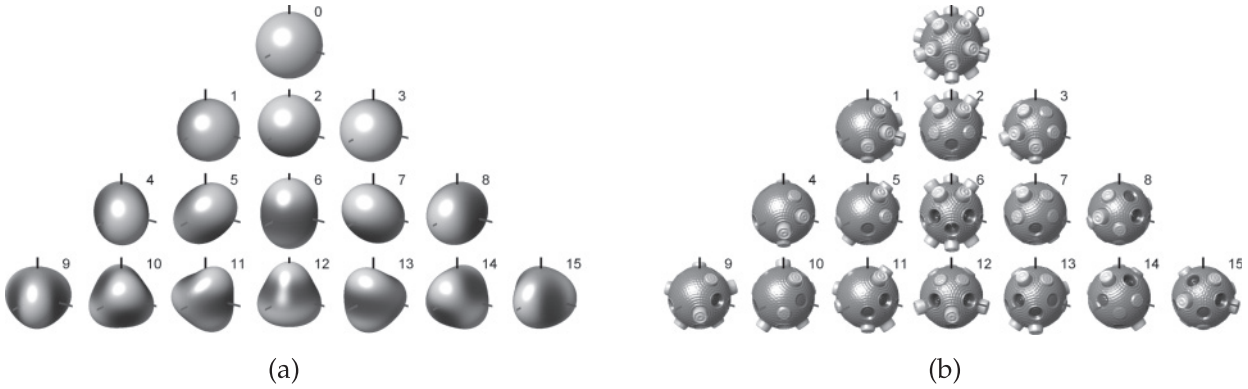

Figure 8

and verification of the filters required to configure the DAW plug-ins. A novel limiting criterion is introduced to safely operate the array by ensuring a limited loudspeaker excursion. The MIMO system design presented here is based on laser Doppler vibrometry measurements. The resulting far-field beam pattern is examined based on microphone-array measurements at a finite distance, and the measured data are extrapolated to the far field to verify the design.

Beamforming with the IKO

The key to controlling focused sound beams with the IKO is the ability to control the sound particle velocity on its surface in the shape of spherical harmonics; see Figure 8a.

The IKO houses 20 passive loudspeakers that are mounted into its rigid faces (shown in Figure 1). Because all loudspeakers of the IKO share one common enclosure volume, the motion of the loudspeaker

Figure 9. MIMO synthesis of spherical harmonic beam patterns.

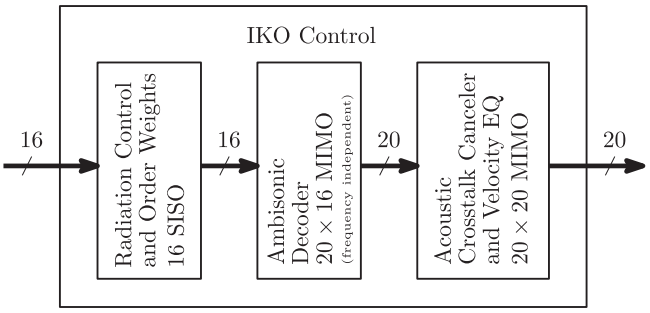

Figure 10. Surface vibration patterns on a sphere are radiated to sound pressure in the far field, with frequency responses depending on the spherical harmonic order n*. The diagram shows these responses for a sphere of the radius* R = *28.5 cm. The far-field sound pressure is characterized by the increasingly strong attenuation of components of high orders and low frequencies, yielding (*n + *1)th-order high-pass slopes, cf. Equation 1.*

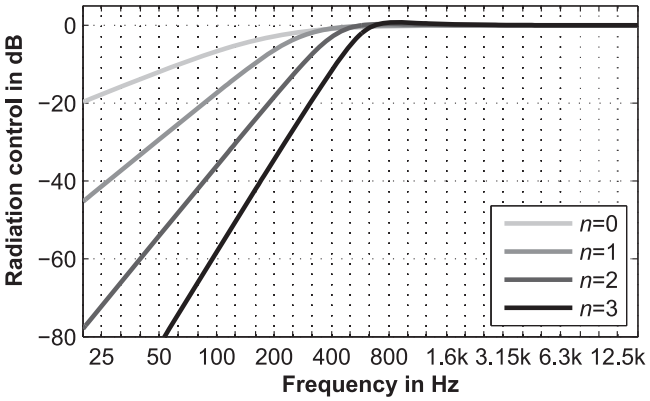

Figure 10

cones is acoustically coupled. Directivity pattern synthesis requires individual control of the cone motions, however, so that a MIMO crosstalk canceler is needed. The vibrometry-based identification of the canceler is described in the section "Measurement and Control of Loudspeaker Cone Velocity," see the rightmost block of the schema in Figure 9.

According to the equations of sound radiation, any surface velocity vibration pattern in the exact shape of an individual spherical harmonic (cf. Figure 8a) propagates to a sound-pressure pattern of the same shape at any radius. The pattern only undergoes a radius- and frequency-dependent change of magnitude and phase, obeying a well-defined frequency response for each order n of spherical harmonic (Zotter 2009). In the far field, this is

$$b_n(k\mathrm{R}) = \frac{\rho c\, \mathrm{i}^n}{k h_n'^{(2)}(k\mathrm{R})}, \qquad (1)$$

where ρ is the density of air (1.2 kg/m^3), c is the speed of sound (343 m/sec), and i is the imaginary unit. The wave number $k = 2\pi f/c$ is defined by the frequency f, and $h_n'^{(2)}(k\mathrm{R})$ is the derivative of the nth-order spherical Hankel function of the second kind that describes radiation for Fourier representations with a positively signed exponent $e^{\mathrm{i}2\pi f t}$ (Zotter 2009). The effective acoustical radius of the IKO is R = 28.5 cm.

Complicated surface vibration patterns are smoothed out as the sound is radiated to the far field. Accordingly, signals decoded to high-order patterns are strongly attenuated, particularly at low frequencies (see Figure 10). The remaining low-order patterns—decoded to the loudspeakers (as seen in Figure 8b) by the signal processing block in the middle of Figure 9—can be equalized by *far-field radiation control* to compensate for the amplitude and phase changes they undergo when radiated (Zotter and Noisternig 2007; Pomberger 2008; Kerscher 2010). This step consists of single-input, single-output filters (SISO) and is accomplished by the leftmost block in Figure 9. This enables one to compose far-field beam patterns out of superimposed low-order spherical harmonics.

Given a suitable control system achieving the control of the IKO's surface velocity and radiation, the composition of far-field beam patterns in terms of spherical harmonics works using the same tools as for arranging sounds in higher-order Ambisonics, i.e., Ambisonic encoding. Figure 11 demonstrates that, for an aiming of a spherical harmonic beam towards the angle 0° on the horizon, the effort to develop elaborated systems pays off: Narrower beams can be achieved maintaining a more consistent shape over a larger frequency range. Figure 11a shows a beam pattern achieved by plain max-r_E Ambisonic amplitude panning (Zotter, Pomberger, and Schmeder 2008; see also Daniel, Rault, and Polack 1998 for details on max-r_E weighting), and Figure 11b displays a system we designed in 2014 (cf. Lösler and Zotter 2015). To avoid audible distortions due to overload at low frequencies, this design entailed the necessity of a low-frequency amendment by crossing over to an omnidirectional subwoofer mode.

Figure 11. Beam pattern of a horizontal beam, with magnitude in dB (grayscale) over polar angle and frequency for spherical harmonic beamforming with the IKO using systems with plain max-r_E Ambisonic amplitude panning (a); a version from 2014 of radiation control including EQ by ear and MIMO acoustic crosstalk cancellation (b); and the new limited-excursion design without MIMO acoustic crosstalk cancellation but EQ for the active loudspeaker velocity (c). Magnitude levels indicated as levels of gray (d).

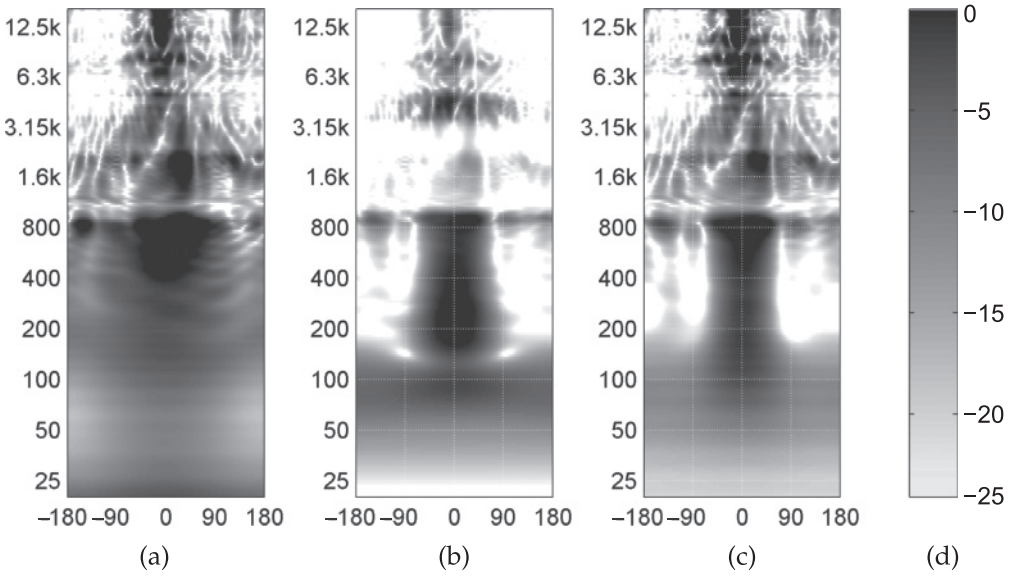

Later in this article, the section "Limiting the Loudspeaker Cone Excursion" will present our new design method recognizing excursion as a more reasonable physical limitation than the white-noise gain constraint, which we had previously used and that was adopted from microphone array theory. Even without a MIMO crosstalk canceler for the IKO's loudspeaker cones, this concept achieves beams that are more focused than in our previous design, whose rough equalization by ear obviously led to a lack of energy above 800 Hz (compare the graphs in Figures 11b and 11c).

Desired max-r_E Beam Patterns

Far-field beam-pattern synthesis by the IKO uses the same description as the angular amplitude patterns in higher-order Ambisonics. The max-r_E beam patterns that will be used here turned out to exhibit sufficiently high side-lobe attenuation while maintaining a narrow main lobe (Daniel, Rault, and Polack 1998). On-axis equalized max-r_E beams of the orders $i \leq \mathrm{N}$ are shown in Figure 12 and described in earlier publications (Zotter and Frank 2012; Lösler and Zotter 2015), giving the equation

$$g_i(\boldsymbol{\theta}) = \sum_{n=0}^{\mathrm{N}} \sum_{m=-n}^{n} Y_n^m(\boldsymbol{\theta})\, w_{n,i}\, Y_n^m(\boldsymbol{\theta}_c), \tag{2}$$

$$w_{n,i} = \begin{cases} \dfrac{P_n\left(\cos\left(\frac{137.9^\circ}{i+1.51}\right)\right)}{\sum_{n=0}^{i}(2n+1)\, P_n\left(\cos\left(\frac{137.9^\circ}{i+1.51}\right)\right)} & \text{for } n \leq i \\ 0 & \text{elsewhere,} \end{cases}$$

where the $Y_n^m(\boldsymbol{\theta})$ are the fully orthonormal spherical harmonics as depicted in Figure 8, and the $P_n(\cdot)$ are nth-order Legendre polynomials (cf. Zotter and Frank 2012). The two direction vectors $\boldsymbol{\theta}$ and $\boldsymbol{\theta}_c$ denote the observed direction of radiation and the adjustable beam direction, respectively. The controllable Ambisonics order is considered to be limited by N, and the weights $w_{n,i}$ are the max-r_E order weights.

The Ambisonic encoding shown in Figure 3 corresponds to the distribution of a single-channel signal to $(\mathrm{N}+1)^2$ channels using the spherical harmonics $Y_n^m(\boldsymbol{\theta}_c)$ evaluated at the beam direction $\boldsymbol{\theta}_c$ as weights, as suggested by the rightmost term in Equation 2. The IKO control system has the task of representing the two leftmost terms, $Y_n^m(\boldsymbol{\theta})$ and

Figure 12. Spherical harmonic max-r_E beam patterns of orders $i = 0, 1, 2, 3$, yielding rotationally symmetrical directivity patterns, which could be drawn as balloon diagrams in three dimensions. Here, the polar diagram shows semicircular generatrix curves in alternation on the interval $[0°, \pm 180°]$ to maintain quantitative legibility.

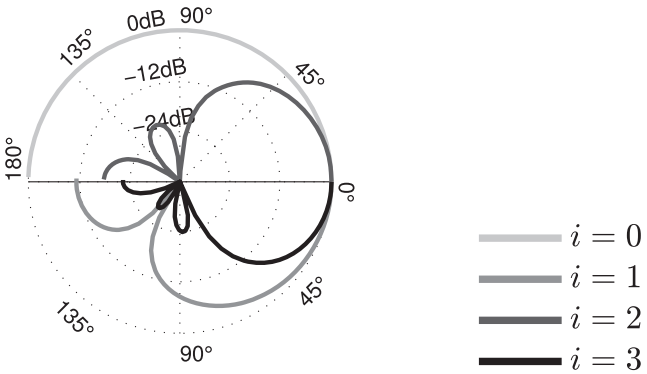

$w_{n,i}$, by achieving the best possible synthesis of all the controllable $(N + 1)^2$ max-r_E-weighted spherical harmonics in the far field.

The highest controllable order N depends on the number of loudspeakers L, with $L \geq (N + 1)^2$. The highest-order pattern for the $L = 20$ of the IKO is $g_3(\boldsymbol{\theta})$ and its synthesis is difficult to accomplish at low frequencies. Instead, reasonable processing produces a sequence of increasingly focused beam patterns $g_0(\boldsymbol{\theta})$, $g_1(\boldsymbol{\theta})$, $g_2(\boldsymbol{\theta})$, $g_3(\boldsymbol{\theta})$ over frequency.

Cap Model of Surface Vibration

A unity-gain velocity excited by the loudspeaker cone sitting at the direction $\boldsymbol{\theta}_l$ can be modeled as a spherical cap of the aperture angle α. For a variable direction of observation, this is expressed as a unit step function $u(\boldsymbol{\theta}^{\mathrm{T}}\boldsymbol{\theta}_l - \cos(\alpha/2))$. Its contribution to each spherical harmonic is defined by the transform

$$\nu_{nm}^{[l]}|_{\mathrm{R}} = \int u\left(\boldsymbol{\theta}^{\mathrm{T}}\boldsymbol{\theta}_l - \cos\frac{\alpha}{2}\right) Y_n^m(\boldsymbol{\theta})\,\mathrm{d}\boldsymbol{\theta},$$

(cf. Zotter, Sontacchi, and Höldrich 2007), yielding

$$\nu_{nm}^{[l]}|_{\mathrm{R}} = a_n\, Y_n^m(\boldsymbol{\theta}_l),$$

$$a_n = \begin{cases} P_{n-1}(\cos\frac{\alpha}{2}) - \cos\frac{\alpha}{2}\, P_n(\cos\frac{\alpha}{2}) & n > 0 \\ 1 - \cos(\frac{\alpha}{2}) & n = 0. \end{cases}$$

A weighted superposition of all the IKO's loudspeaker cones, assuming their velocities are given by the weights v_l, is written as

$$\nu_{nm}|_{\mathrm{R}} = a_n \sum_{l=1}^{\mathrm{L}} Y_n^m(\boldsymbol{\theta}_l)\, v_l.$$

We can stack the $(N + 1)^2$ coefficients of spherical harmonics $\nu_{nm}|_{\mathrm{R}}$ into a vector $\boldsymbol{\nu}_{\mathrm{N}} = [\nu_{nm}]$ and the L loudspeaker velocities of the IKO into another vector $\boldsymbol{v} = [v_l]$. The a_n weights, written as vector $\boldsymbol{a}_{\mathrm{N}} = [a_n]$, and the spherical harmonics up to the order N sampled at the 20 loudspeakers, written as matrix $\boldsymbol{Y}_{\mathrm{N}} = [Y_n^m(\boldsymbol{\theta}_l)]_{nm}^l$, permit us to express the matrix equation as $\boldsymbol{\nu}_{\mathrm{N}}|_{\mathrm{R}} = \mathrm{diag}\{\boldsymbol{a}_{\mathrm{N}}\}\boldsymbol{Y}_{\mathrm{N}}\,\boldsymbol{v}$ whose least-squares inverse

$$\boldsymbol{v} = \underbrace{\boldsymbol{Y}_{\mathrm{N}}^{\mathrm{T}}\left(\boldsymbol{Y}_{\mathrm{N}}\boldsymbol{Y}_{\mathrm{N}}^{\mathrm{T}}\right)^{-1}}_{:=\boldsymbol{D}_{\mathrm{N}}} \mathrm{diag}\{\boldsymbol{a}_{\mathrm{N}}\}^{-1}\ \boldsymbol{\nu}_{\mathrm{N}}|_{\mathrm{R}}$$

yields suitable loudspeaker velocities. Expressed in its scalar form, with the decoder coefficients $\boldsymbol{D}_{\mathrm{N}} = [d_{nm}^{[l]}]$, the loudspeaker velocities v_l producing the coefficients $\nu_{nm}|_{\mathrm{R}}$ are

$$v_l = \sum_{n=0}^{\mathrm{N}} \sum_{m=-n}^{n} \frac{d_{nm}^{[l]}}{a_n}\, \nu_{nm}|_{\mathrm{R}}. \qquad (3)$$

Radiation Control

As specified by $b_n(k\mathrm{R})$ in the frequency domain (cf. Equation 1 and Figure 10), the spherical harmonic coefficient of the surface velocity $\nu_{nm}|_{\mathrm{R}}$ radiates into the far field, yielding the sound-pressure coefficient

$$\psi_{nm} = b_n(k\mathrm{R})\, \nu_{nm}|_{\mathrm{R}}.$$

The aim is to control this coefficient to obtain a far-field beam pattern as in Equation 2

$$\psi_{nm} = Y_n^m(\boldsymbol{\theta}_c)\, w_{n,i},$$

so we invert the equation to obtain

$$\nu_{nm}|_{\mathrm{R}}(f, \boldsymbol{\theta}_c) = \frac{w_{n,i}}{b_n(k\mathrm{R})}\, Y_n^m(\boldsymbol{\theta}_c).$$

Insertion into Equation 3 yields the loudspeaker velocities required to produce the desired max-r_E

beam pattern $g_i(\boldsymbol{\theta})$, here with $i = 0, 1, 2, 3$,

$$v_l^{[i]}(f, \boldsymbol{\theta}_c) = \sum_{n=0}^{\mathrm{N}} \sum_{m=-n}^{n} \frac{d_{nm}^{[l]}}{a_n} \frac{w_{n,i}}{b_n(k\mathrm{R})} Y_n^m(\boldsymbol{\theta}_c).$$

Figure 10 shows that the inverse of $b_n(k\mathrm{R})$ can require unrealistic bass boosts to compensate for attenuation of higher orders. For spherical microphone arrays, realistic implementations consider filtering into successive frequency bands $H_i(f)$, in which only an increasingly focused beam pattern $g_i(\boldsymbol{\theta})$ is synthesized with $i = 0, 1, 2, 3$ (Lösler and Zotter 2015). Summed over these bands, the required loudspeaker velocities become

$$v_l(f, \boldsymbol{\theta}_c) = \sum_{n=0}^{\mathrm{N}} \sum_{m=-n}^{n} d_{nm}^{[l]} \sum_{i=0}^{\mathrm{N}} \underbrace{\frac{H_i(f)}{a_n} \frac{w_{n,i}}{b_n(k\mathrm{R})}}_{:=H_{i,n}(f)} Y_n^m(\boldsymbol{\theta}_c). \quad (4)$$

The radiation control filters obtained in this way, $H_{i,n}(f)$, depend on the spherical harmonic order n and the synthesized beam order i. The question is how to design the filters $H_i(f)$ they contain to comply with physical limitations.

Limiting the Loudspeaker Cone Excursion

In microphone arrays, white-noise gain limitation prevents self-noise amplification (Lösler and Zotter 2015). For loudspeaker arrays, the limiting relates instead to a maximum linear transducer excursion $|x_l| \leq \mathrm{x}_{\max}$. Excursion is defined by integrating velocity over time. Accordingly, we formulate the constraint in the frequency domain

$$\max_{l,\boldsymbol{\theta}_c} |x_l(f, \boldsymbol{\theta}_c)| \leq \mathrm{x}_{\max}$$

using $x_l(f, \boldsymbol{\theta}_c) = v_l(f, \boldsymbol{\theta}_c)/\mathrm{i}2\pi f$.

The original radiation control filters $1/b_n(k\mathrm{R})$ exhibit slopes proportional to $1/f^{n+1}$. By the additional factor $1/\mathrm{i}2\pi f$, slopes for unlimited excursion are proportional to $1/f^{n+2}$. Hence, high-pass filters stabilizing the individual radiation control filters by enforcing a constant excursion limit must at least be proportional to f^{n+2}. What is more, whenever such an excursion limit takes effect, the magnitude of the corresponding radiation pattern will vanish in the far field. To exclusively drive excursions producing audible sounds, economic use of excursion requires limitation filters of slopes proportional to f^{n+3}, at least. We define the following filter bank using zero-phase high- and low-pass filters:

$$\hat{H}_0(f) = \frac{(f/f_0)^3}{1+(f/f_0)^3} \frac{1}{1+(f/f_1)^4},$$

$$\hat{H}_1(f) = \frac{(f/f_1)^4}{1+(f/f_1)^4} \frac{1}{1+(f/f_2)^5},$$

$$\hat{H}_2(f) = \frac{(f/f_2)^5}{1+(f/f_2)^5} \frac{1}{1+(f/f_3)^6},$$

$$\hat{H}_3(f) = \frac{(f/f_3)^6}{1+(f/f_3)^6}.$$

To make these filters complementary in amplitude to an overall high-pass filter

$$H_{\mathrm{sum}}(f) = \frac{(f/f_0)^3}{1+(f/f_0)^3},$$

they are normalized using

$$H_i(f) = \frac{(f/f_0)^3}{1+(f/f_0)^3} \frac{\hat{H}_i(f)}{\sum_{i=0}^{\mathrm{N}} \hat{H}_i(f)}.$$

Inserted into Equation 4, with suitable cut-on frequencies f_i, the filters yield limited excursion curves as show in Figure 13b, where the excursion was normalized by the excursion reached at 40 Hz in omnidirectional radiation mode (dashed line).

Measurement and Control of Loudspeaker Cone Velocity

This section deals with measuring the voltage-to-velocity transfer functions of the IKO's loudspeakers, including acoustic coupling (crosstalk) between active and passive movements of the loudspeaker cones. The measured matrix is used to design an equalized and crosstalk-canceled control system for loudspeaker velocities. The voltage-to-velocity transfer functions of the 20 loudspeakers were

Figure 13. Filter bank $H_i(f)$ *and overall response using suitably chosen cut-on frequencies* $[f_i]^T = [40, 70, 113, 173]$ *Hz (a), and the resulting limited excursion normalized at 40 Hz (b).*

Figure 14. Active voltage-to-velocity responses of all 20 loudspeakers (a), and 19 passive responses to excitation voltages at loudspeaker 1 out of $\mathbf{T}(f) = [t_{ij}(f)]$ *(b).*

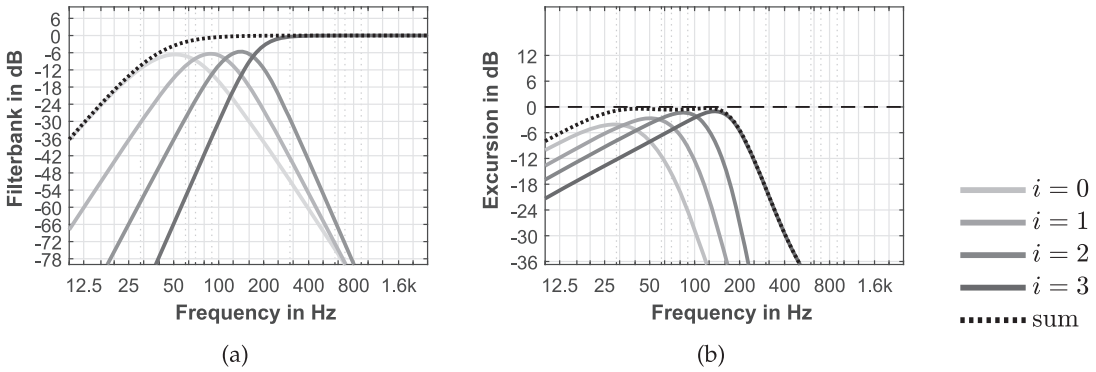

(a) (b)

Figure 13

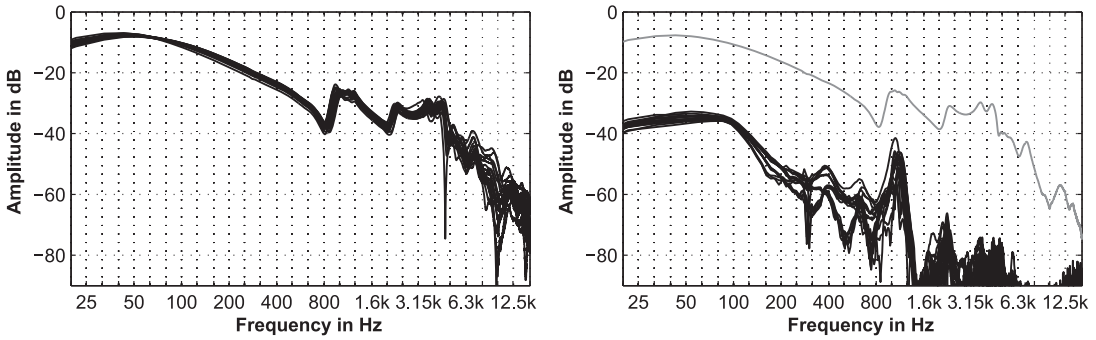

(a) (b)

Figure 14

measured using the exponential sine-sweep method (Farina 2000) and a laser Doppler vibrometer along the cone axis, approximately 24 cm away from each loudspeaker (as shown in Figure 5a). All measured impulse responses were cropped to 4,096 samples at a 44.1-kHz sample rate. Figure 14 shows some frequency responses.

With the transfer-function matrix in the frequency domain $\boldsymbol{T}$, the output velocities $\boldsymbol{v} = [v_1, \ldots, v_L]^T$ caused by the input voltages $\boldsymbol{u} = [u_1, \ldots, u_L]^T$ are calculated as

$$\boldsymbol{v} = \boldsymbol{T}\,\boldsymbol{u}.$$

The frequency dependency is omitted from this notation to maintain simplicity. Given that $\boldsymbol{T}$ is invertible, decoupled cone velocities $\boldsymbol{v}$ are controlled by the voltages

$$\boldsymbol{u} = \boldsymbol{T}^{-1}\,\boldsymbol{v},$$

and one can insert Equation 4 for beamforming. To keep the corresponding impulse responses short and easy to window in the time domain, a regularized inverse $\boldsymbol{T}^H(\boldsymbol{T}\boldsymbol{T}^H + a\,\frac{\mathrm{tr}\{\boldsymbol{T}\boldsymbol{T}^H\}}{L}\boldsymbol{I})^{-1}$ was used, with $L = 20$. The regularization was set to $a = 0.1$.

The 20×20 voltage-to-velocity impulse responses are available at http://phaidra.kug.ac.at/o:37716.

Verification by Sound Pressure Measurements

Verification of whether the far-field beam pattern complies with the desired max-r_E beam pattern

Figure 15. Horizontal cuts through the on-axis direction of far-field beam patterns of IKO, using a MIMO crosstalk canceler and limited-excursion radiation control. Using polar angle and frequency as axes, the diagrams show dB values for three beam directions: on-axis direction of loudspeaker 6 (a); direction between loudspeakers 6, 11, and 15 (b); and directions between loudspeakers 6 and 11 (c). Magnitude levels are indicated as levels of gray (d).

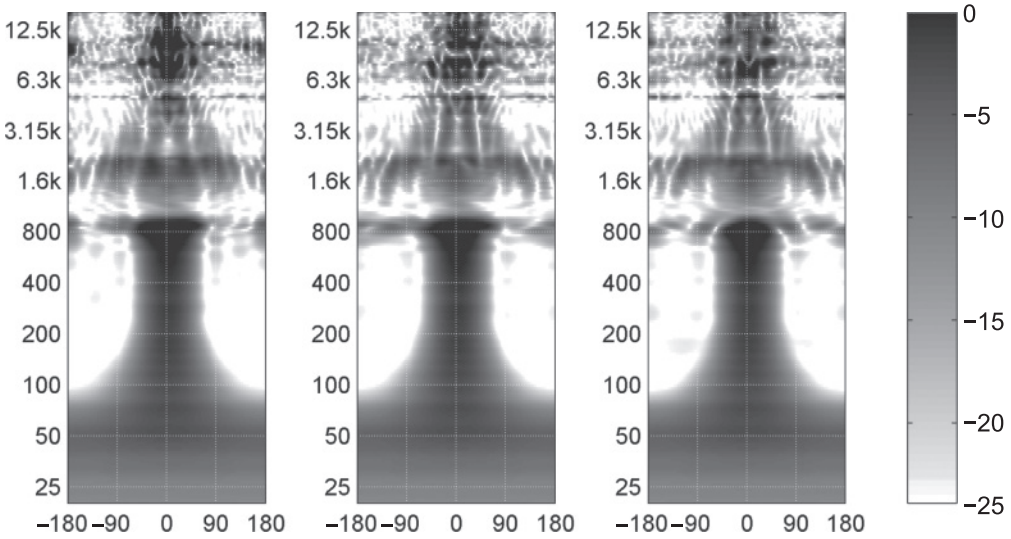

has been achieved by microphone measurements surrounding the IKO, as shown in Figure 5b (cf. also Zotter and Bank 2012). The impulse responses of the loudspeaker-to-microphone paths were also measured using the exponential sine-sweep technique and windowing to 320 samples. A sine-square fade-in of 20 samples was used before the first impulse and an 80-sample fade-out at the very end.

The 648 × 20 voltage-to-sound-pressure impulse responses are available at http://phaidra.kug.ac.at/o:37715.

In the frequency domain, the sound-pressure sample $p_j|_{75\ \mathrm{cm}}$ received at the jth microphone due to the driving voltages u_l from each of the loudspeakers is described by the transfer paths $g_{lj}(f)$ of a MIMO system,

$$p_j|_{75\ \mathrm{cm}}(f) = \sum_{l=1}^{\mathrm{L}} g_{lj}(f)\, u_l. \tag{5}$$

The least-square-error inverse

$$\boldsymbol{C} = (\boldsymbol{Y}\boldsymbol{Y}^{\mathrm{T}})^{-1}\, \boldsymbol{Y}^{\mathrm{T}} = [c_{nm}^{(j)}]$$

of $\boldsymbol{Y} = [Y_{nm}(\boldsymbol{\theta}_j)]$ (the spherical harmonics sampled at the microphone positions $\boldsymbol{\theta}_j$) permits decomposition into coefficients of spherical harmonics $\psi_{nm}|_{75\ \mathrm{cm}}$ up to $n \le 17$ with the given measurement setup.

The far-field sound pressure is calculated from this decomposition at a desired cross section

$$p_{\mathrm{ff}}(f, \boldsymbol{\theta}) = \sum_{n=0}^{17} \sum_{m=-n}^{n} \frac{\mathrm{i}^{n+1}\, Y_n^m(\boldsymbol{\theta})}{k\, h_n(k 75\ \mathrm{cm})} \sum_{j=1}^{648} c_{nm}^{(j)}\, p_j|_{75\ \mathrm{cm}}(f).$$

Figure 15 shows a cross section centered on beams with different orientations after inserting the IKO control into Equation 5. The new beam patterns are more constant and narrow in the range from 150 Hz to 800 Hz than they were with earlier approaches.

At 200 Hz, the previous approaches in Figure 11 yield beams reaching an attenuation of approximately −6 dB from their maximum at angles between ±135° (Figure 11a), ±60° (Figure 11b), ±50° (Figure 11c), and the proposed filter design in Figure 15 reaches this value at ±45°. At 100 Hz, the proposed design achieves a ±70-degree width for a −6 dB attenuation from its maximum. With the previous designs, only the design in Figure 11c achieved focus at all to ±80°, but it was not able to maintain the amplitude below 100 Hz.

The new beam patterns in Figure 15 become roughly omnidirectional below 100 Hz, and above 800 Hz the inherent spatial aliasing counteracts a smooth beam pattern. A notch around 1 kHz appears, most probably because of a mismatch of

the loudspeaker cone vibration from an ideally rigid shape. Around the frequencies 1.6 kHz, 5 kHz, and 8 kHz, the IKO seems to lose its directivity. This is probably caused by modal breakup or interior modes of the IKO.

Conclusion

We presented the IKO, a new computer music instrument utilizing superdirective spherical harmonic beamforming to orchestrate the wall reflections in a room. We could outline its use by free, ready-to-use DAW plug-ins enabling its spherical harmonic beamforming in real time, and its use as a virtualized instrument (vIKO) that is freely available together with illustrative binaural renderings. We gave a precise description of our IKO prototype and basic concert setups that were used in the past.

To describe perceptual aspects of the spherical harmonic beamforming with the IKO, we reviewed previous experiments and showed new results indicating that the IKO allows one to control the direction as well as the distance impression of the synthesized sound objects.

We summarized the spherical harmonic beamforming theory of compact spherical arrays and presented a simple way of defining a bank of linear-phase limitation filters that suppress side lobes in each of its frequency bands. We were able to outline constraints that are relevant for compact spherical loudspeaker arrays, since the more common white-noise-gain limitations, as applicable to spherical microphone arrays, become meaningless in this context.

Finally, we presented a practical study to measure responses to design an entire multiple-input, multiple-output control filter set. It is based on laser Doppler vibrometry measurements for a clean control of the IKO's loudspeaker cone velocities, with crosstalk cancelled; excursion-limited analytic filter design, suppressing side lobes, for radiation control; and measurements verifying the synthesized radiation patterns by using far-field extrapolated measurements with a spherical microphone array. All measurement data are made available to support reproducible research.

Acknowledgments

This work was funded by the Austrian Science Fund (FWF), project no. AR 328-G21, "Orchestrating Space by Icosahedral Loudspeaker." We would like to thank *Computer Music Journal*'s anonymous reviewers and Editor, and Frank Schultz of sonible, for their valuable comments on our manuscript.

References

Avizienis, R., et al. 2006. "A Compact 120 Independent Element Spherical Loudspeaker Array with Programmable Radiation Patterns." In *Proceedings of the 120th Audio Engineering Society Convention*. Available online at www.aes.org/e-lib/browse.cfm?elib=13587 (subscription required). Accessed April 2017.

Bennett, M. B., and D. T. Blackstock. 1975. "Parametric Array in Air." *Journal of the Acoustical Society of America* 57(3):562–568.

Bloch, A., R. Medhurst, and S. Pool. 1953. "A New Approach to the Design of Super-Directive Aerial Arrays." *Proceedings of the IEE-Part III: Radio and Communication Engineering* 100(67):303–314.

Boulez, P. 1983. "L'Acoustique et la musique contemporaine: Introduction." In *Revue d'acoustique: Congrès international d'acoustique*, pp. 213–216.

Brandstein, M., and D. Ward. 2001. *Microphone Arrays: Signal Processing Techniques and Applications*. Berlin: Springer.

Butler, J. L., and S. L. Ehrlich. 1977. "Superdirective Spherical Radiator." *Journal of the Acoustical Society of America* 61(6):1427–1431.

Caussé, R., J. Bresciani, and O. Warusfel. 1992. "Radiation of Musical Instruments and Control of Reproduction with Loudspeakers." In *Proceedings of the International Symposium on Musical Acoustics*, pp. 67–70.

Cook, P., et al. 1998. "N>>2: Multi-Speaker Display Systems for Virtual Reality and Spatial Audio Projection." In *Proceedings of the International Conference on Auditory Display*. Available online at www.icad.org/Proceedings. Accessed 21 March 2017.

Croft, J. J., and J. O. Norris. 2003. "Theory, History, and the Advancement of Parametric Loudspeakers: A Technology Overview." Technical Report 98-10006-1100 Rev. E. San Diego, California: American Technology Corporation.

Daniel, J., J.-B. Rault, and J.-D. Polack. 1998. "Ambisonics Encoding of Other Audio Formats for Multiple Listening

Conditions." In *Proceedings of the 105th Audio Engineering Society Convention*. Available online at www.aes.org/e-lib/browse.cfm?elib=8385 (subscription required). Accessed April 2017.
Elko, G. W. 2000. "Superdirectional Microphone Arrays." In J. Benesty and S. L. Gay, eds. *Acoustic Signal Processing for Telecommunication*. Berlin: Kluwer.
Farina, A. 2000. "Simultaneous Measurement of Impulse Response and Distortion with a Swept-Sine Technique." In *Proceedings of the 108th Audio Engineering Society Convention*. Available online at www.aes.org/e-lib/browse.cfm?elib=10211 (subscription required). Accessed April 2017.
Frank, M., G. K. Sharma, and F. Zotter. 2015. "What We Already Know about Spatialization with Compact Spherical Arrays as Variable-Directivity Loudspeakers." Paper presented at the inSonic Conference, 26–28 November, Karlsruhe, Germany. Available online at iem.kug.ac.at/fileadmin/media/osil/2015_FrankEtAl_inSonic_WhatWeAlreadyKnowAboutSpatializationWithCompactSphericalArraysAsVariabledirectivityLoudspeakers.pdf. Accessed March 2017.
Kassakian, P. 2005. "Magnitude Least-Squares Fitting via Semidefinite Programming with Applications to Beamforming and Multidimensional Filter Design." In *Proceedings of the IEEE International Conference onAcoustics, Speech, and Signal Processing*. Available online at ieeexplore.ieee.org/document/1415644 (subscription required). Accessed May 2017.
Kassakian, P. 2006. "Convex Approximation with Applications in Magnitude Filter Design and Beamforming." PhD dissertation, Electrical Engineering and Computer Science, University of California, Berkeley. Available online at www2.eecs.berkeley.edu/Pubs/TechRpts/2006/EECS-2006-64.pdf. Accessed March 2017.
Kassakian, P., and D. Wessel. 2003. "Design of Low-Order Filters for Radiation Synthesis." In *Proceedings of the 115th Audio Engineering Society Convention*. Available online at www.aes.org/e-lib/browse.cfm?elib=12448 (subscription required). Accessed April 2017.
Kassakian, P., and D. Wessel. 2004. "Characterization of Spherical Loudspeaker Arrays." In *Proceedings of the 117th Audio Engineering Society Convention*. Available online at www.aes.org/e-lib/browse.cfm?elib=12940 (subscription required). Accessed April 2017.
Kerscher, M. 2010. *Compact Spherical Loudspeaker Array, Implementation of a System for Variable Sound Radiation*. Saarbrücken: VDM.
Kronlachner, M. 2014. "Plug-in Suite for Mastering the Production and Playback in Surround Sound and Ambisonics." Paper presented at the 136th Audio Engineering Society Convention Student Design Competition, 28 April 2014, Berlin. Available online at www.matthiaskronlachner.com/wp-content/uploads/2013/01/kronlachner_aes_studentdesigncompetition_2014.pdf. Accessed March 2017.
Laitinen, M.-V., et al. 2015. "Controlling the Perceived Distance of an Auditory Object by Manipulation of Loudspeaker Directivity." *Journal of the Acoustical Society of America* 137(6):462–468.
Lindemann, W. 1986. "Extension of a Binaural Cross-Correlation Model by Contralateral Inhibition: I. Simulation of Lateralization for Stationary Signals." *Journal of the Acoustical Society of America* 80(6):1608–1622.
Lösler, S., and F. Zotter. 2015. "Comprehensive Radial Filter Design for Practical Higher-Order Ambisonic Recording." In *Fortschritte der Akustik: Tagungsband der deutschen Arbeitsgemeinschaft für Akustik*, pp. 452–455.
Miranda, L., D. Cabrera, and K. Stewart. 2013. "A Concentric Compact Spherical Microphone and Loudspeaker Array for Acoustical Measurements." In *Proceedings of the 135th Audio Engineering Society Convention*. Available online at www.aes.org/e-lib/browse.cfm?elib=16986 (subscription required). Accessed April 2017.
Misdariis, N., et al. 2001. "Radiation Control on Multi-Loudspeaker Device: La Timée." In *Proceedings of the International Computer Music Conference*, pp. 306–309.
Morgenstern, H., B. Rafaely, and F. Zotter. 2015. "Theory and Investigation of Acoustic Multiple-Input Multiple-Output Systems Based on Spherical Arrays in a Room." *Journal of the Acoustical Society of America* 138(5):2998–3009.
Morgenstern, H., F. Zotter, and B. Rafaely. 2012. "Joint Spherical Beam Forming for Directional Analysis of Reflections in Rooms." *Journal of the Acoustical Society of America* 131(4):3207–3207.
Pasqual, A. M. 2010. "Sound Directivity Control in a 3-D Space by a Compact Spherical Loudspeaker Array." PhD dissertation, University of Campinas, Faculty of Mechanical Engineering, Campinas, Brazil.
Pasqual, A. M., J. R. Arruda, and P. Herzog. 2010. "Application of Acoustic Radiation Modes in the Directivity Control of a Spherical Loudspeaker Array." *Acta Acustica United with Acustica* 96(1):32–42.
Pasqual, A. M., P. Herzog, and J. R. Arruda. 2010. "Theoretical and Experimental Analysis of the Behavior of a Compact Spherical Loudspeaker Array for Directivity

Control." *Journal of the Acoustical Society of America* 128(6):3478–3488.
Poletti, M. A., T. Betlehem, and T. D. Abhayapala. 2015. "Higher-Order Loudspeakers and Active Compensation for Improved 2D Sound Field Reproduction in Rooms." *Journal of the Audio Engineering Society* 63(1–2):31–45.
Pollow, M. 2014. "Directivity Patterns for Room Acoustical Measurements and Simulations." PhD dissertation, RWTH-Aachen, Institute of Technical Acoustics.
Pollow, M., and G. K. Behler. 2009. "Variable Directivity for Platonic Sound Sources Based on Spherical Harmonics Optimization." *Acta Acustica United with Acustica* 95(6):1082–1092.
Pomberger, H. 2008. "Angular and Radial Directivity Control for Spherical Loudspeaker Arrays." Master's thesis, University of Music and Performing Arts, Institute of Electronic Music and Acoustics, Graz, Austria.
Rafaely, B., and D. Kaykin. 2011. "Optimal Model-Based Beamforming and Independent Steering for Spherical Loudspeaker Arrays." *IEEE Transactions on Audio Speech and Language Processing* 19(7):2234–2238.
Rakerd, B., W. M. Hartmann, and J. Hsu. 2000. "Echo Suppression in the Horizontal and Median Sagittal Planes." *Journal of the Acoustical Society of America* 107(2):1061–1064.
Schelkunoff, S. A. 1943. "A Mathematical Theory of Linear Arrays." *The Bell System Technical Journal* 22(1):80–107.
Sharma, G. K. 2016. "Composing with Sculptural Sound Phenomena in Computer Music." PhD dissertation, University of Music and Performing Arts, Institute of Electronic Music and Acoustics, Graz, Austria.
Sharma, G. K., F. Zotter, and M. Frank. 2014. "Orchestrating Wall Reflections in Space by Icosahedral Loudspeaker: Findings from First Artistic Research Exploration." In *Proceedings of the Joint International Computer Music Conference and the Sound and Music Computing Conference*, pp. 830–835.
Sugibayashi, Y., et al. 2012. "Three-Dimensional Acoustic Sound Field Reproduction Based on Hybrid Combination of Multiple Parametric Loudspeakers and Electrodynamic Subwoofer." *Applied Acoustics* 73(12):1282–1288.
Takumai, S. 2006. "Loudspeaker Array Device and Method for Setting Sound Beam of Loudspeaker Array Device." WIPO patent WO 2,006,001,272 A1, filed 21 June 2005, and granted 5 January 2006.
Trueman, D., et al. 2006. "PLOrk: The Princeton Laptop Orchestra, Year 1." In *Proceedings of the International Computer Music Conference*, pp. 443–450.
Warusfel, O., P. Derogis, and R. Caussé. 1997. "Radiation Synthesis with Digitally Controlled Loudspeakers." In *Proceedings of the 103rd Audio Engineering Society Convention*. Available online at www.aes.org/e-lib/browse.cfm?elib=7202 (subscription required). Accessed April 2017.
Wendt, F., et al. 2016. "Directivity Patterns Controlling the Auditory Distance." In *Proceedings of the International Conference on Digital Audio Effects*, pp. 295–300.
Wendt, F., et al. 2017. "Perception of Spatial Sound Phenomena Created by the Icosahedral Loudspeaker." *Computer Music Journal* 41(1):76–88.
Zaunschirm, M., M. Frank, and F. Zotter. 2016. "An Interactive Virtual Icosahedral Loudspeaker Array." In *Fortschritte der Akustik: Tagungs-CD der deutschen Arbeitsgemeinschaft für Akustik*, pp. 1331–1334.
Zotter, F. 2009. "Analysis and Synthesis of Sound-Radiation with Spherical Arrays." PhD dissertation, University of Music and Performing Arts, Institute of Electronic Music and Acoustics, Graz, Austria.
Zotter, F., and B. Bank. 2012. "Geometric Error Estimation and Compensation in Compact Spherical Loudspeaker Array Calibration." In *Proceedings of the IEEE International Instrumentation and Measurement Technology Conference*, pp. 2710–2715.
Zotter, F., and M. Frank. 2012. "All-Round Ambisonic Panning and Decoding." *Journal of the Audio Engineering Society* 60(10):807–820.
Zotter, F., and M. Frank. 2015. "Investigation of Auditory Objects Caused by Directional Sound Sources in Rooms." *Acta Physica Polonica A* 128(1-A):5–10.
Zotter, F., and R. Höldrich. 2007. "Modeling Radiation Synthesis with Spherical Loudspeaker Arrays." In *Proceedings of the International Congress on Acoustics*. Available online at iem.kug.ac.at/fileadmin/media/iem/altdaten/projekte/publications/paper/modeling_radiation/modeling.pdf. Accessed 21 March 2017.
Zotter, F., and M. Noisternig. 2007. "Near- and Far-Field Beamforming Using Spherical Loudspeaker Arrays." In *Congress of the Alps Adria Acoustics Association*. Available online at iem.kug.ac.at/fileadmin/media/iem/altdaten/projekte/publications/paper/near/near.pdf. Accessed 21 March 2017.
Zotter, F., H. Pomberger, and A. Schmeder. 2008. "Efficient Directivity Pattern Control for Spherical Loudspeaker Arrays." In *Proceedings of the Joint Meeting of the Acoustical Society of America and the European Acoustics Association*. Available online at

iem.kug.ac.at/fileadmin/media/iem/altdaten/projekte/publications/paper/efficient/efficient.pdf. Accessed March 2017.
Zotter, F., and A. Sontacchi. 2007. "Icosahedral Loudspeaker Array." Technical Report IEM Report 39/07. University of Music and Performing Arts, Institute of Electronic Music and Acoustics.
Zotter, F., A. Sontacchi, and R. Höldrich. 2007. "Modeling a Spherical Loudspeaker System as Multipole Source." In *Fortschritte der Akustik: Tagungsband der deutschen Arbeitsgemeinschaft für Akustik*, pp. 221–222.
Zotter, F., et al. 2014. "Preliminary Study on the Perception of Orientation-Changing Directional Sound Sources in Rooms." In *Proceedings of the Forum Acusticum*. Paper presented at the Forum Acusticum, 7–12 September, Krakow, Poland. Available online at ambisonics.iem.at/Members/zotter/2014_zotter_OrientationDirectionalSource.pdf. Accessed March 2017.